Solid State Communications, Vol.40, pp.843-846.
Pergamon Press Ltd. 1981. Printed in Great Britain.

0038-1098/81/450843-04$02.00/0

A STUDY OF NON-THERMALIZED LUMINESCENCE SPECTRA: THE CASE OF Cu_2O

N. Caswell

Department of Physics, University of California
Berkeley, California 94720

J. S. Weiner and P. Y. Yu

Department of Physics, University of California and
Materials and Molecular Research Division
Lawrence Berkeley Laboratory, Berkeley, California 94720

(Received July 14, 1981 by M. Cardona)

The emission spectra of a non-thermalized distribution of excitons in Cu_2O have been studied experimentally and theoretically. The emission spectra were found to exhibit interesting dependence on both the excitation frequencies and on the sample temperatures. These experimental results are explained quantitatively by a simple model calculation of the exciton distribution in Cu_2O under continuous excitation. Using this model the exciton non-radiative lifetime was deduced from the emission spectra. In addition, the present theory accounts for the lineshape of the resonant Raman peaks in Cu_2O more satisfactorily than the existing theory.

In this letter we report a detailed experimental and theoretical investigation of photon emission due to non-thermalized excitons in Cu_2O. Phenomena associated with a non-thermal equilibrium distribution of carriers occur in many semiconductors. In particular, such effects are well known in the photoluminescence spectra of amorphous[1] and heavily doped[2] semiconductors and in the polariton fluorescence spectra of high purity semiconductors.[3] So far most of these emission spectra have not been quantitatively analyzed because of the unknown parameters involved. This is unfortunate, since such spectra contain potentially interesting information which would otherwise be lost during the thermalization of the carriers. Cu_2O is chosen for this study because its emission spectrum has many of the features common to the more complex systems while its properties are well known. The theory can be compared with experiment using a minimum number of adjustable parameters and from these parameters the exciton non-radiative lifetime and effective mass can be deduced. In addition, the present theory resolves the discrepancy between experiment and the previous theory of Yu and Shen[4] (hitherto referred to as YS) with regard to the lineshape of some resonant Raman peaks in Cu_2O.

Before presenting our results we briefly review the relevant properties of Cu_2O.[4-10] Cu_2O forms a cubic crystal with space group O_h^4, two molecules per unit cell and 15 optical phonons: 87 cm^{-1} (Γ_{25}^-), 110 cm^{-1} (Γ_{12}^-), 152 cm^{-1} ($\Gamma_{15}^{-(1)}$(TO)), 153 cm^{-1} ($\Gamma_{15}^{(1)}$(LO)), 350 cm^{-1}(Γ_2^-), 515 cm^{-1} (Γ_{25}^+), 633 cm^{-1} ($\Gamma_{15}^{-(2)}$(TO)), and 662 cm^{-1} ($\Gamma_{15}^{-(2)}$(LO)). The crystal has inversion symmetry so all states have definite parity. The exciton formed from the top valence band (Γ_7^+) and the bottom conduction band (Γ_6^+) is referred to as the yellow exciton. The 1S bound state of the yellow exciton is split by the exchange interaction into a Γ_{25}^+ triplet state (orthoexction) with frequency 16400 cm^{-1} and a Γ_2^+ singlet (paraexciton) state at 16304 cm^{-1}. Optical excitation of either state by an electric-dipole transition is forbidden by parity but phonon-assisted dipole transitions are allowed for odd parity optical phonons. For the paraexciton dipole transitions are allowed only with the assistance of the Γ_{25}^- optical phonon, while transitions are allowed for the orthoexciton with any of the listed odd parity phonons. Of these transitions, the one involving the Γ_{12}^- phonon is found to be at least ten times stronger than transitions involving the other optical phonons or the paraexciton. This dominance of the Γ_{12}^- phonon has been explained by the proximity of the Γ_{12}^- conduction band which serves as the dipole allowed intermediate state.

The photoluminescence spectra of Cu_2O due to the yellow 1S orthoexciton are shown in Fig. 1. In both curves the excitation frequencies are well above the Γ_{12}^- phonon-assisted indirect absorption edge at 16509 cm^{-1}. Although these spectra have been reproduced from Ref. 6, we have obtained similar spectra on our samples. The sharp line at 16400 cm^{-1} labelled as E_1 in Ref. 6 is due to direct electric-quadrupole recombination of the orthoexciton. The broader peak labelled B is due to Γ_{12}^- phonon-assisted dipole recombination of the exciton. As pointed out in Ref. 6, the peak B has two different lineshapes depending on the sample preparation procedure.

Samples showing a spectrum similar to the one in Fig. 1(a) are believed to be of good quality, while samples with a spectrum similar to the one shown in Fig. 1(b) are believed to have many defects.

In Fig. 1(a), the lineshape of the B peak is quantitatively explained by assuming that the excitons are in thermal equilibrium with each other. The exciton distribution function, $\rho_k(E)$, is assumed to be given by the Boltzmann distribution function, $\exp(-E/kT_{ex})$, where k is the Boltzmann constant and T_{ex} is the exciton temperature. Notice that T_{ex} may be different from the bath temperature. In Ref. 6, the lineshape of the B peak was fitted with the following expression for the luminescence intensity $I(\omega_s)$:

$$I(\omega_s) \propto g(E)\rho_k(E) \qquad (1)$$

where the exciton kinetic energy E is related to the emission frequency ω_s by $\hbar\omega_s = E_o + E - \hbar\omega_{12}$. E_o and $\hbar\omega_{12}$ are respectively the zone-center exciton and Γ_{12}^- phonon energies. g(E) is the exciton density-of-states and was assumed to be proportional to $E^{\frac{1}{2}}$ by Petroff et al.[6] The points in Fig. 1(a) are a plot of Eq. (1) with $T_{ex} = 7°K$ while the bath temperature is 1.8°K. The agreement between theory and experiment is quite satisfactory. Also, the emission lineshape was found to be temperature dependent but independent of the excitation frequency as would be expected from a system in thermal equilibrium.

On the other hand, the lineshape of the B peak in Fig. 1(b) cannot be fitted satisfactorily by Eq. (1) with a Boltzmann distribution function. The points in Fig. 1(b) are representative of such a fit with T_{ex} adjusted to a rather large value of 26°K. In addition, we have found that this emission spectrum is rather insensitive to sample temperature for temperature below 77°K. Also, as the excitation frequency approaches the indirect absorption edge so that the B peak now overlaps the $2\Gamma_{12}^-$ Raman peak, the width of the peak B narrows because its intensity at frequencies above the $2\Gamma_{12}^-$ Raman peak decreases. Some representative experimental spectra are shown as solid curves in Fig. 2. The sharp structures in Fig. 2 whose emission frequencies vary with the excitation frequency have been identified as resonant Raman peaks in YS.

It has been proposed that the behavior of exciton emission spectra as represented by curves in Fig. 1(b) and in Fig. 2 is due to a non-thermalized exciton distribution caused by an exciton non-radiative lifetime too short for the excitons to attain thermal equilibrium.[2,6] Although this explanation accounts qualitatively for the increased linewidth and lower integrated intensity of the exciton emission in samples with a large number of defects (presumably due to oxygen complexes in Cu_2O), so far this theory has not been tested quantitatively. In this paper we show for the first time that such a theory can indeed account quantitatively for all the experimental results for Cu_2O.

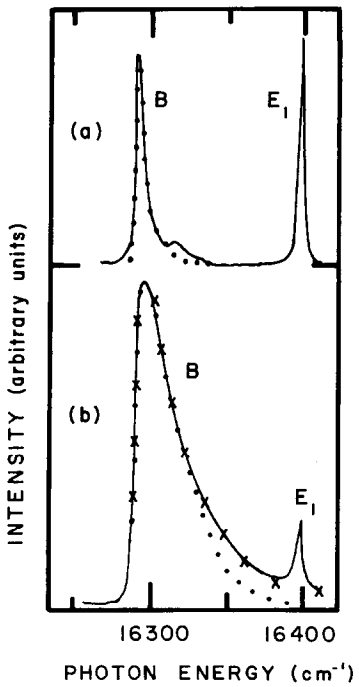

Fig. 1. The luminescence spectra of the yellow 1S or orthoexciton in Cu_2O at 1.8°K for (a) a sample grown by an arc image furnace and (b) a sample grown by oxidation of copper. The solid curves are the experimental curves from Ref. 6. The solid circles are fits with a Boltzmann distribution and exciton temperatures $T_{ex} = 7°K$ and 26°K respectively for (a) and (b). The points denoted by 'x' are calculated with the model discussed in the text.

In order to calculate the non-thermalized luminescence spectra in Fig. 1(b) and Fig. 2, we first obtain the exciton distribution function $\rho_k(E)$ from the following rate equation:

$$\left(\frac{d\rho_k}{dt}\right) = \left(\frac{\partial\rho_k}{\partial t}\right)_{in} - \left(\frac{\partial\rho_k}{\partial t}\right)_{out} + \left(\frac{\partial\rho_k}{\partial t}\right)_c - \left(\frac{\partial\rho_k}{\partial t}\right)_r - \left(\frac{\partial\rho_k}{\partial t}\right)_{nr} \qquad (2)$$

where k is the exciton vector. $\left(\frac{\partial\rho_k}{\partial t}\right)_{in}$ and $\left(\frac{\partial\rho_k}{\partial t}\right)_{out}$ represent, respectively, the rates at which excitons are scattered into and out of the state k by phonons. $\left(\frac{\partial\rho_k}{\partial t}\right)_c$ is the rate of exciton creation due to the incident radiation. $\left(\frac{\partial\rho_k}{\partial t}\right)_r$ is the exciton radiative recombination rate while $\left(\frac{\partial\rho_k}{\partial t}\right)_{nr}$ is the non-radiative rate due to defects plus the net conversion rate of orthoexcitons into paraexcitons.[11]

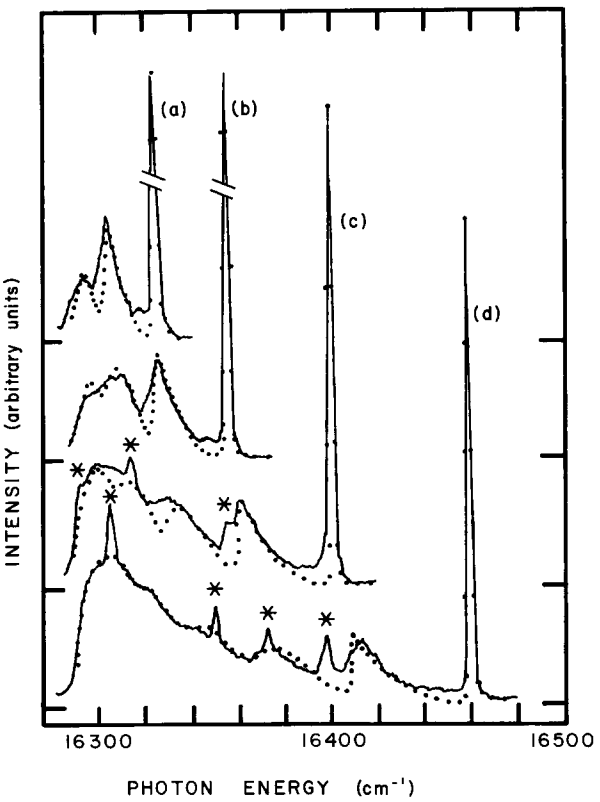

Fig. 2. Luminescence spectra in Cu_2O at ~ 2.1 K as a function of the excitation frequencies: (a) 16547 cm^{-1}, (c) 16620 cm^{-1} and (d) 16678 cm^{-1}. The solid curves are the experimental results while the solid circles are calculated from our model. Peaks denoted as * are due to phonons not included in the present model (see YS for their identifications).

We numerically solve Eq. (2) for the steady state solution (i.e., $\frac{d\rho_k}{dt} = 0$) utilizing the following assumptions based on previous optical results:[4,5]

(i) The kinetic energy of the exciton is given by: $E = \hbar^2k^2/2m$, where m is its effective mass.

(ii) Interactions between the exciton and optical phonons other than the Γ_{12}^- mode can be neglected.

(iii) The Γ_{12}^- phonon is dispersionless.[12]

(iv) The scattering of excitons by the transverse acoustic phonon is negligible compared to scattering by the longitudinal acoustic (LA) phonon. The exciton-LA phonon interaction matrix element is assumed to be proportional to the phonon wave vector q. The constant of proportionality depends on the deformation potential and other quantities, which are known for Cu_2O.

(v) The LA phonon dispersion is isotropic and is given by $\omega_{LA} = vq$, where v is the LA phonon velocity.

(vi) $\left(\frac{\partial\rho_k}{\partial t}\right)_r$ and $\left(\frac{\partial\rho_k}{\partial t}\right)_{nr}$ are both independent of k and furthermore $\left(\frac{\partial\rho_k}{\partial t}\right)_{nr} \gg \left(\frac{\partial\rho_k}{\partial t}\right)_r$.

Our model can be schematically represented by Fig. 3. Excitons are created by indirect absorption of the incident photon (ω_i) at energy $E_c = \hbar\omega_i - \hbar\omega_{12} - E_o$. Those excitons which radiatively recombine without scattering by LA phonons produce the sharp $2\Gamma_{12}^-$ Raman line at $\omega_s = \omega_i - 2\omega_{12}$ described in YS. The rest will either decay non-radiatively or be scattered by LA phonons. Since the exciton-LA phonon interaction matrix element increases with the phonon wave vector q, peaks appear in ρ_k at multiples of vq_{max} below E_c where q_{max} is the maximum q allowed by energy and momentum conservation. These produce the asymmetric peaks below the

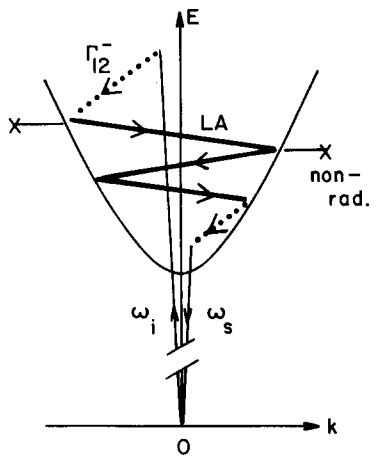

Fig. 3. Schematic description of processes included in our calculation of the exciton distribution function. The light arrows denote optical transitions, the dotted arrows denote exciton scattering by Γ_{12}^- phonons while the heavy arrows denote exciton scattering by LA phonons. Non-radiative recombinations are represented by a line terminated by an x.

$2\Gamma_{12}^-$ Raman line in the spectra in Fig. 2 and identified as LA phonon sidebands of the $2\Gamma_{12}^-$ Raman peak in YS. In this simple model, the difference between thermalized and non-thermalized emission spectra is due entirely to the magnitude of the phonon scattering terms relative to $\left(\frac{\partial\rho_k}{\partial t}\right)_{nr}$. The phonon scattering terms lead to the establishment of thermal equilibrium among the excitons. However, if $\left(\frac{\partial\rho_k}{\partial t}\right)_{nr}$ is comparable or larger than the phonon scattering rates, then excitons cannot thermalize before they recombine.

To obtain the theoretical curves shown as points in Fig. 2 and as x's in Fig. 1(b), the exciton creation rate is assumed to be a delta function $\delta(E - E_c)$. The scattering rate $\left(\frac{\partial \rho_k}{\partial t}\right)_{out}$ is obtained by summing the probability of scattering an exciton out of a given initial state into all possible final states. The rate $\left(\frac{\partial \rho_k}{\partial t}\right)_{in}$ is obtained by summing the corresponding probability over all initial states. For the exciton-LA phonon matrix element of Cu_2O we use the deformation potential of 2.1eV determined by Trebin et al.[9] Calculation of $\left(\frac{\partial \rho_k}{\partial t}\right)_{in}$ and $\left(\frac{\partial \rho_k}{\partial t}\right)_{out}$ also involves a kinematic factor mv^2, which determines the position of the subsidiary phonon sideband peaks in Fig. 2. We have determined m to be 2.7 ± 0.1 times the free electron mass m_e. YS found a slightly higher value of $3.0m_e$, but this difference is within the experimental uncertainty. Other than for m and an overall intensity scale factor, $\left(\frac{\partial \rho_k}{\partial t}\right)_{nr}$ is then the only adjustable parameter in the calculation. The theoretical curves in Fig. 1(b) and Fig. 2 are obtained by setting $\left(\frac{\partial \rho_k}{\partial t}\right)_{nr}$ equal to $(3.5 \pm 0.5) \times 10^{10} sec^{-1}$ and convoluting the spectra calculated with Eqs. (1) and (2) by a Gaussian spectrometer spectral function (FWHM = 2 cm^{-1}).

Other than for the small peaks labelled '*', which are due to phonons not considered here, the theory reproduces very well all the salient features of the experimental spectra including those previously identified as due to resonant Raman scattering in YS. In fact, YS found that their theoretical lineshapes of the $2\Gamma_{12}^- + nLA$ (n = 1 and 2) Raman modes are wider than those experimentally observed while we do not find such discrepancy between our theory and experiment. We conclude that this is because they have arbitrarily decomposed the spectrum into Raman peaks and a luminescence background. Our results show that in Cu_2O it is not necessary to spearate the two because our model includes both in a simple unified manner.[13] We also note the excellent agreement between our theory and the non-thermalized luminescence lineshape in Fig. 1(b). This is the first time such a lineshape has been explained quantitatively for Cu_2O. The thermalized emission spectrum in Fig. 1(a) can be obtained also in our model by simply decreasing $\left(\frac{\partial \rho_k}{\partial t}\right)_{nr}$.

In fact, our model predicts a continuous transition from a non-thermalized spectrum to a thermalized spectrum by simply reducing $\left(\frac{\partial \rho_k}{\partial t}\right)_{nr}$ relative to the phonon scattering rates. Experimentally, we have been able to observe this transition by increasing the phonon scattering rate by increasing the sample remperature. This temperature dependence of the emission spectra will be published elsewhere. Another feature of our model is that it predicts quantitatively the temporal evolution of the shape of the emission spectra excited by a picosecond laser pulse. We are now in the process of observing this experimentally with a modelocked dye laser. Finally, we note that $\left(\frac{\partial \rho_k}{\partial t}\right)_{nr}$ for Cu_2O has also been determined by Habiger and Compaan[14] by analyzing the width of the E_1 quadrupole transition in Fig. 1. Their value of 2.4×10^{10} sec^{-1} is in good agreement with our result.

Acknowledgement: This work was started when one of us (NC) was an IBM postdoctoral fellow at Berkeley and was supported by a grant from the Research Corporation, the National Science Foundation Grant No. DMR7919463, and by the Director, Office of Energy Research, Office of Basic Energy Sciences, Materials Sciences Division of the U.S. Department of Energy under Contract No. W-7405-ENG-48.

REFERENCES

1. SHAH, J. and BÖSCH, M. A., Phys. Rev. Lett. 42, 1420 (1979).
2. PERMOGOROV, S. and TRAVNIKOV, V., Solid State Commun. 29, 615 (1979).
3. See references in SUMI, H., J. Phys. Soc. Jpn. 41, 526 (1976).
4. YU, P. Y. and SHEN, Y. R., Phys. Rev. B 12, 1377 (1975).
5. See, for example, NIKITINE, S. in Optical Properties of Solids, edited by S. Nudelman and S. S. Mitra (Plenum, New York, 1969).
6. PETROFF, Y., YU, P. Y. and SHEN, Y.R., Phys. Rev. B 12, 2488 (1975).
7. BLOCH, P. and SCHWAB, C., Phys. Rev. Lett. 41, 514 (1978).
8. FRÖHLICH, D., KENBLIES, R., UIHLEIN, CH. and SCHWAB, C., Phys. Rev. Lett. 43, 1260 (1979).
9. TREBIN, H. R., CUMMINS, H. Z. and BIRMAN, J. L., Phys. Rev. B 23, 597 (1981); WATERS, R.G., POLLACK, F. H., BRUCE, R. H. and CUMMINS, H. Z., Phys. Rev. B 21, 1665 (1980).
10. DAHL, J. P. and SWITENDICK, A. C., J. Phys. Chem. Solids 27, 931 (1966).
11. MYSYROWICZ, A., HULIN, D. and ANTONETTI, A., Phys. Rev. Lett. 43, 1123 (1979).
12. BEG, M. M. and SHAPIRO, S. M., Phys. Rev. B 13, 1728 (1976).
13. KLEIN, M. V., Phys. Rev. B 8, 919 (1973). According to this reference, what we calculate here would be called hot luminescence.
14. HABIGER, R. M. and COMPANN, A., Solid State Commun. 26, 533 (1978).